

### Supporting Information

## New Cyclometallated Ru(II) Complex for Potential Application in Photochemotherapy

Bryan A. Albani,<sup>§</sup> Bruno Peña,<sup>†</sup> Kim R. Dunbar,<sup>†,\*</sup> Claudia Turro<sup>§,\*</sup>

<sup>§</sup> Department of Chemistry and Biochemistry, The Ohio State University, Columbus, OH

<sup>†</sup> Department of Chemistry, Texas A&M University, College Station, TX

**Table S1.** Crystal Structural Data and Refinement Parameters for [Ru(biq)<sub>2</sub>(phpy)][PF<sub>6</sub>]<sub>2</sub>•2CH<sub>2</sub>Cl<sub>2</sub> (**1**)

Formula	C <sub>49</sub> H <sub>36</sub> N <sub>5</sub> F <sub>6</sub> Cl <sub>4</sub> PRu
Formula weight	1082.67
Crystal size/mm <sup>3</sup>	0.37 x 0.14 x 0.10
Temperature/K	291(2)
Crystal system	Monoclinic
Space group	<i>P</i> 2 <sub>1</sub> / <i>n</i> (No. 14)
<i>a</i> /Å	13.314(3)
<i>b</i> /Å	22.497(5)
<i>c</i> /Å	15.709(3)
$\beta$ /deg	100.67(3)
<i>V</i> /Å <sup>3</sup>	4623.8(16)
<i>Z</i>	4
$\rho_{\text{calc}}$ /g•cm <sup>-3</sup>	1.555
<i>F</i> <sub>000</sub>	2184
$\mu$ /cm <sup>-1</sup>	0.671
Theta range for data collection/°	1.60 to 27.40
Reflexions collected	49647
Independent reflexions	10375 [ <i>R</i> <sub>int</sub> = 0.0609]
Data/parameters/restraints	10375/595/0
Completeness to theta max/%	98.8
Final <i>R</i> indexes [ <i>I</i> > 2σ( <i>I</i> )]	<i>R</i> 1 <sup><i>a</i></sup> = 0.0637, <i>wR</i> 2 <sup><i>b</i></sup> = 0.1918
Final <i>R</i> indexes [all data]	<i>R</i> 1 <sup><i>a</i></sup> = 0.0828, <i>wR</i> 2 <sup><i>b</i></sup> = 0.2107
Goodness-of-fit on <i>F</i> <sup>2</sup>	1.075

$$^a R1 = \sum ||F_o| - |F_c|| / \sum |F_o|. \quad ^b wR2 = [ \sum [w(F_o^2 - F_c^2)^2] / \sum [w(F_o^2)^2] ]^{1/2}$$

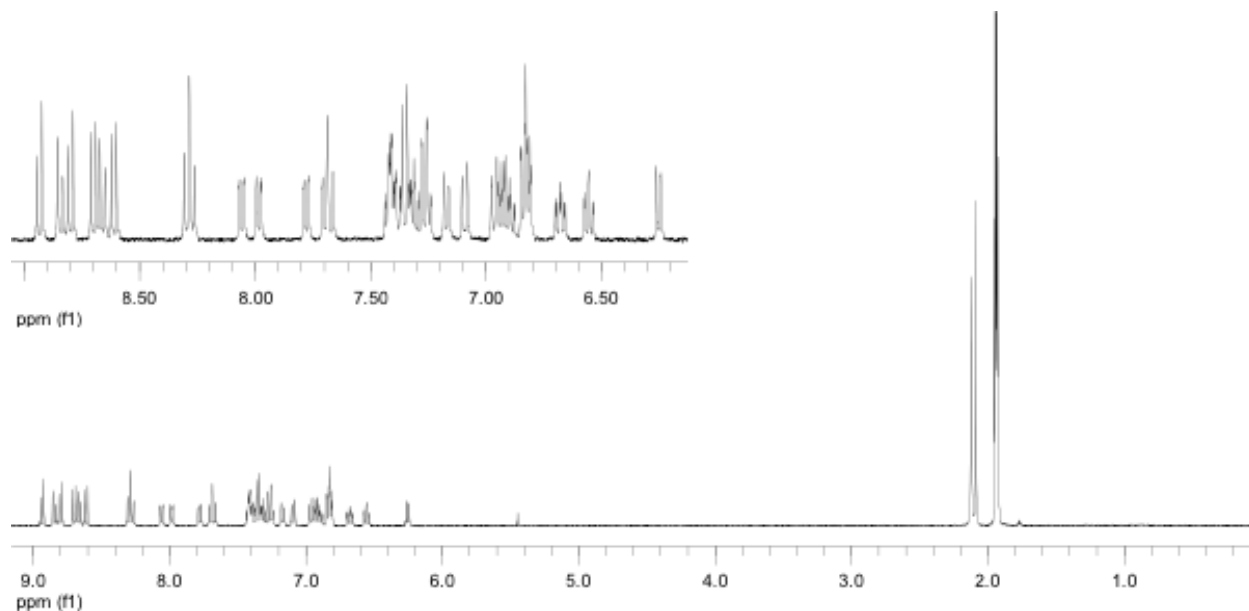


**Figure S1.**  $^1\text{H}$  NMR of **1** in  $\text{CD}_3\text{CN}$ . There are 25 aromatic resonances that correspond to 32 protons.

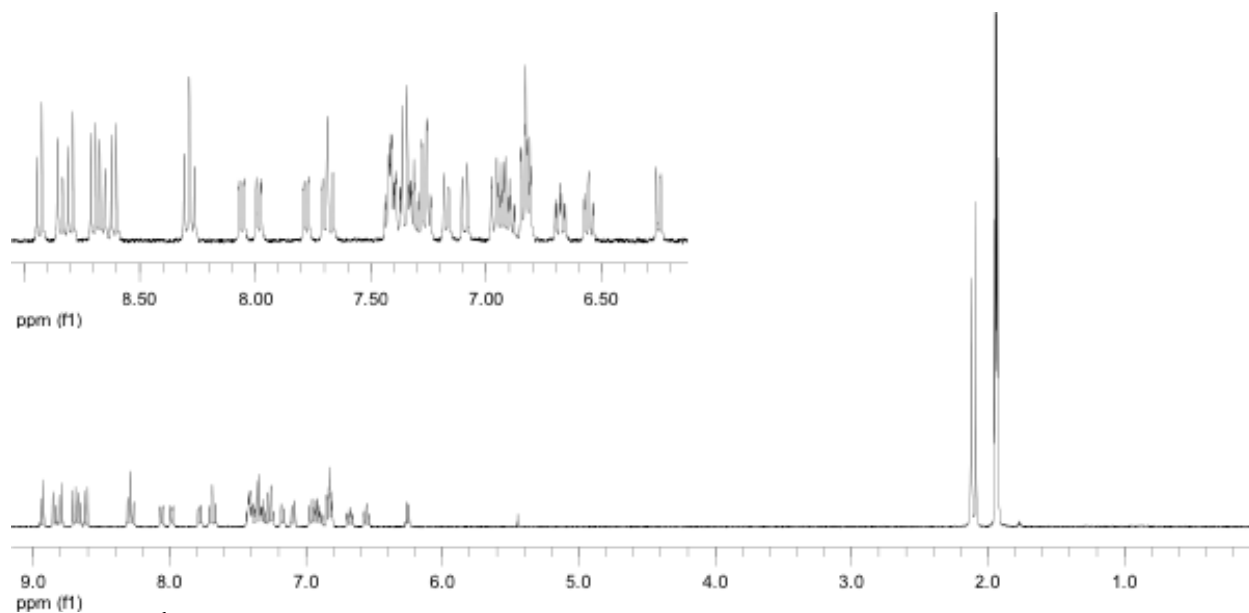


**Figure S2.**  $^1\text{H}$  NMR of **2** in  $(\text{CD}_3)_2\text{CO}$ . There are 14 aromatic resonances that correspond to 32 protons.

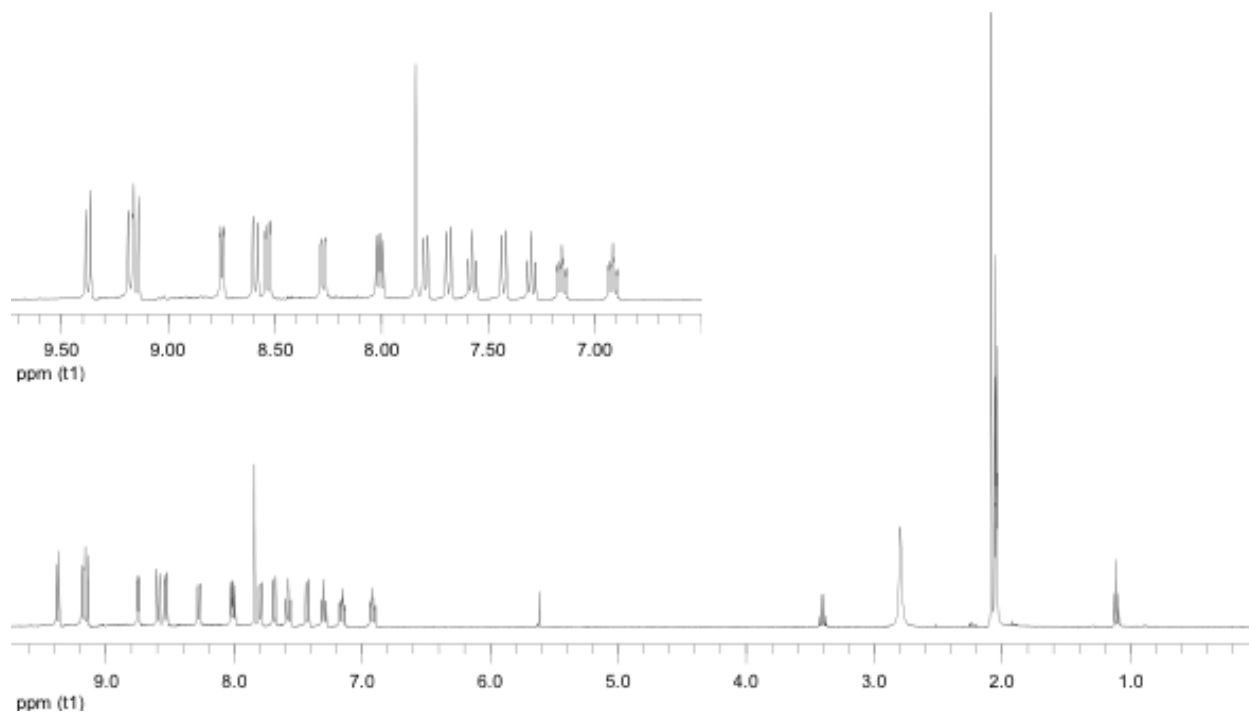


**Figure S3.**  $^1\text{H}$  NMR of **3** in  $(\text{CD}_3)_2\text{CO}$ . There are 15 aromatic resonances that correspond to 32 protons.

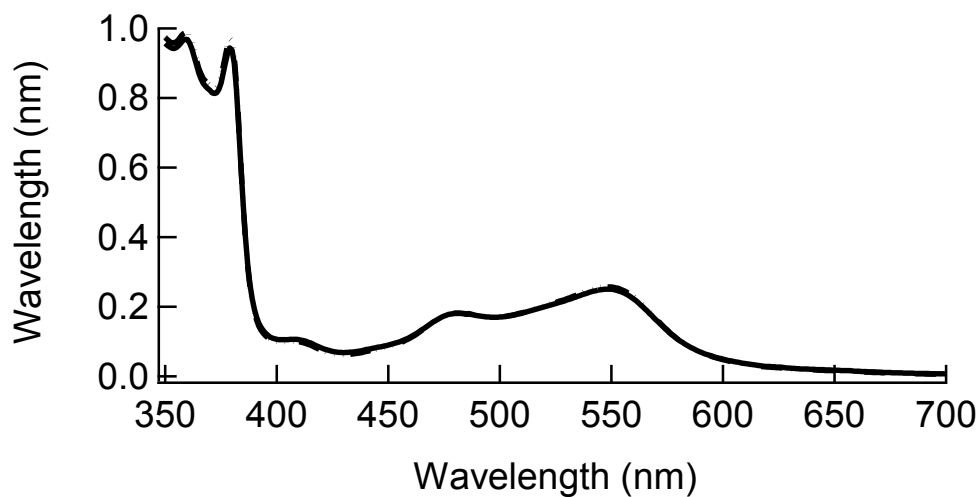


**Figure S4.** Changes to the electronic absorption spectrum of **2** ( $20\ \mu\text{M}$ ) incubated in  $\text{H}_2\text{O}$  for 3 hours at room temperature.

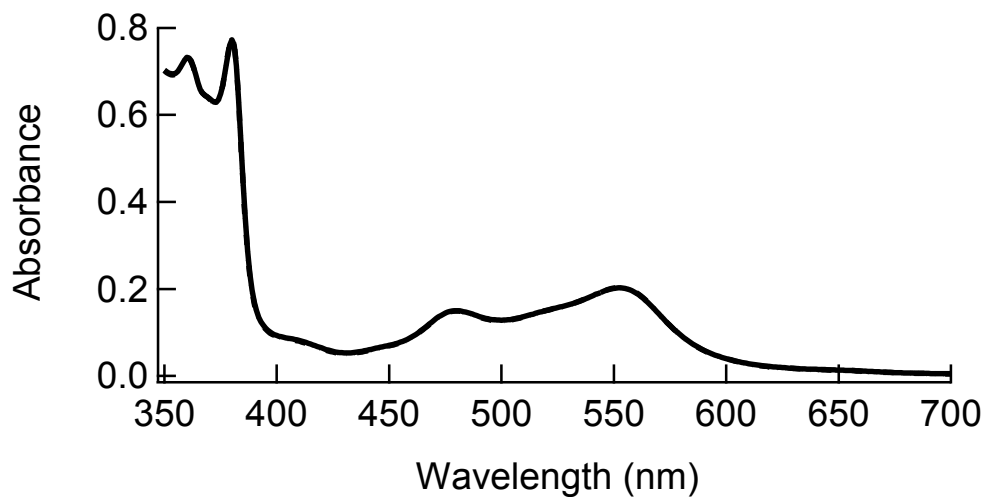


**Figure S5.** Changes to the electronic absorption spectrum of **3** (20 μM) incubated in H<sub>2</sub>O for 3 hours at room temperature.

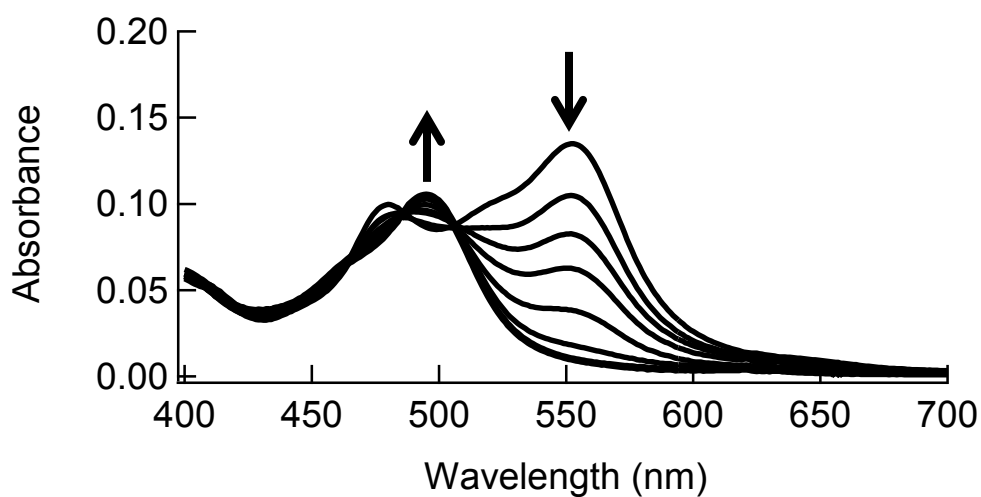


**Figure S6.** Changes to the electronic absorption spectrum of **3** (15 μM) in CH<sub>3</sub>CN with increasing irradiation times: 0, 1, 2, 3, 5, 10, 20, and 30 min ( $\lambda_{\text{irr}} \geq 530$  nm).

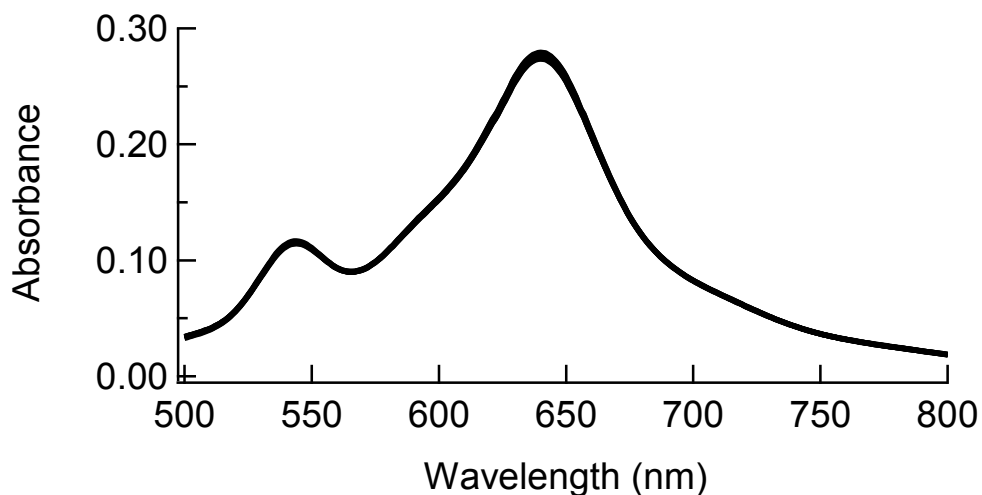


**Figure S7.** Changes to the electronic absorption spectrum of **1** (50  $\mu\text{M}$ ) in  $\text{CH}_3\text{CN}$  with increasing irradiation times: 0, 1, 5, 10, 20, and 30 min ( $\lambda_{\text{irr}} \geq 530$  nm).

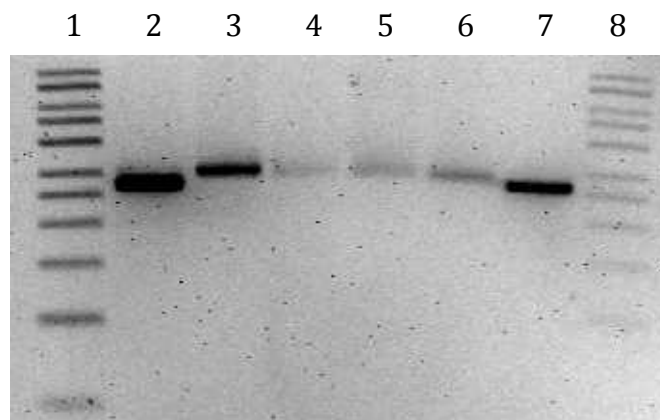


**Figure S8.** Imaged ethidium bromide stained agarose gels in 1xTBE buffer of 50  $\mu\text{M}$  linearized pUC18 plasmid (10mM phosphate buffer, pH = 7.8) in the presence of various concentrations of **3**: lanes 1 and 8, 1 kb DNA molecular weight standard; lanes 2 and 7, linearized plasmid alone; lanes 3-6, 25, 50, 75, 100  $\mu\text{M}$  complex irradiated with  $\lambda_{\text{irr}} \geq 630$  nm ( $t_{\text{irr}} = 30$  min).

**Table S2.** 10 lowest energy singlet excited states obtained from DFT calculations, and the transitions associated with these states in CH<sub>3</sub>CN (H = HOMO, L = LUMO) for complex **1**.

Wavelength (nm)	<i>f</i>	Calculated Transitions and Orbital Contributions <sup>a</sup>
839.53	0.0013	H→L(88%), H→L+1(8%)
765.85	0.0004	H→L+1(86%), H→L(9%), H-1→L+1(2%)
686.27	0.0266	H-1→L(83%), H-2→L(13%)
636.97	0.0288	H-2→L(46%), H-2→L+1(23%), H-1→L+1(18%), H-1→L(10%)
606.78	0.0397	H-2→L(39%), H-1→L+1(29%), H-2→L+1(26%)
537.81	0.0336	H-2→L+1(42%), H-1→L+1(41%), H→L+3(7%)
461.97	0.0068	H→L+2(52%), H→L+4(43%)
455.84	0.0122	H→L+4(46%), H→L+2(39%), H→L+3(10%)
438.86	0.0396	H→L+3(76%), H→L+2(5%)
418.32	0.0302	H-1→L+2(85%), H-1→L+4(5%)

<sup>a</sup>Only contribution ≥5% are listed.

**Table S3.** 10 lowest energy singlet excited states obtained from DFT calculations, and the transitions associated with these states in CH<sub>3</sub>CN (H = HOMO, L = LUMO) for complex **2**.

Wavelength (nm)	<i>f</i>	Calculated Transitions and Orbital Contributions <sup>a</sup>
586.3	0.0003	H→L(97%)
560.87	0.00004	H→L+1(90%), H-1→L+1(4%)
522.69	0.0762	H-1→L(93%)
514.61	0.0041	H-2→L(96%)
491.68	0.0126	H-2→L+1(90%), H-1→L(5%)
476.43	0.0013	H→L+2(97%)
467.09	0.0527	H-1→L+1(76%), H-2→L+2(6%), H→L+1(6%)
439.47	0.0015	H-1→L+2(96%)
404.76	0.0388	H-2→L+2(85%)
389.55	0.005	H-3→L(95%)

<sup>a</sup>Only contribution ≥5% are listed.

**Table S4.** 10 lowest energy singlet excited states obtained from DFT calculations, and the transitions associated with these states in CH<sub>3</sub>CN (H = HOMO, L = LUMO) for complex **3**.

Wavelength (nm)	<i>f</i>	Calculated Transitions and Orbital Contributions <sup>a</sup>
587.43	0.0004	H→L(98%)
550.42	0.0002	H→L+1(89%)
527.23	0.0026	H-2→L(96%)
526.72	0.0862	H-1→L(96%)
493.16	0.0037	H-2→L+1(93%)
467.2	0.0008	H→L+2 (97%)
464.34	0.0657	H-1→L+1(75%), H-2→L+2(7%), H→L+1(6%)
435.34	0.0006	H-2→L+2(97%)
420.11	0.0005	H→L+3(72%), H-2→L+2(22%)
399.83	0.0208	H-1→L+3(37%), H-3→L+2(33%), H→L+3(19%)

<sup>a</sup>Only contribution ≥5% are listed.

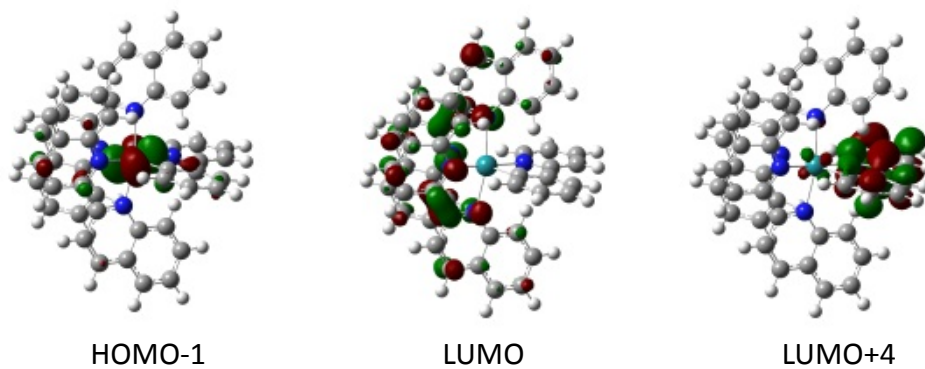


**Figure S9.** Surface images of select molecular orbitals in **1**.

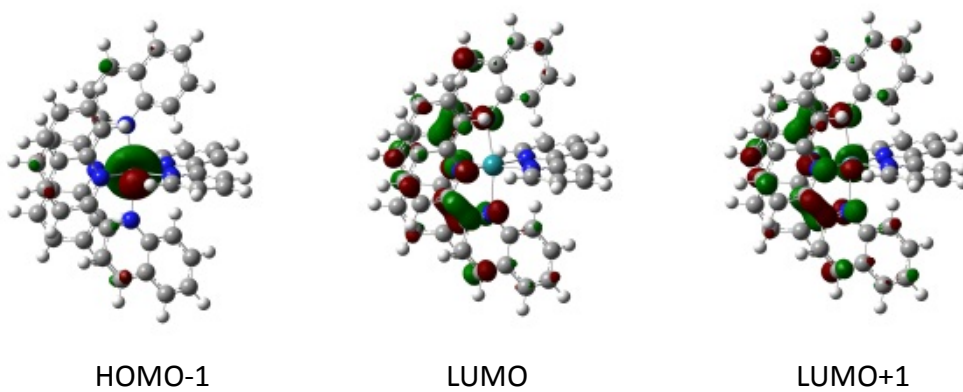


**Figure S10.** Surface images of select molecular orbitals in **2**.

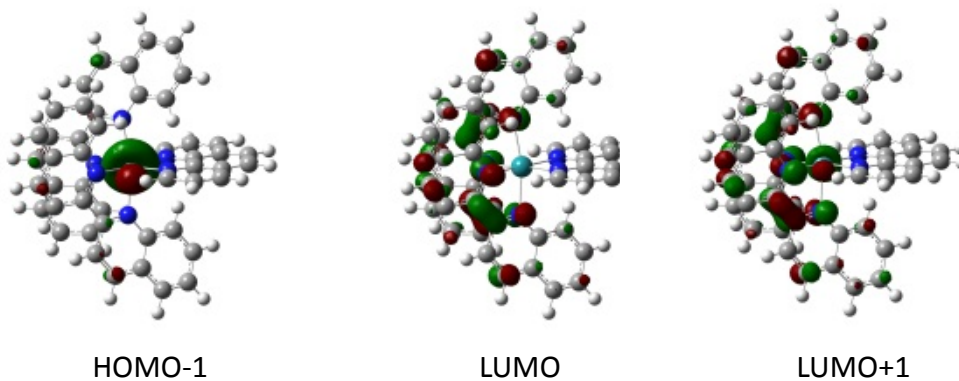


**Figure S11.** Surface images of select molecular orbitals in **3**.